Available online at www.sciencedirect.com
ScienceDirect
Journal of Nuclear Materials 372 (2008) 106–113
journal of nuclear materials
www.elsevier.com/locate/jnucmat

Comparison of TSSD results obtained by differential scanning calorimetry and neutron diffraction

D. Khatamian [a,*], J.H. Root [b]

[a] Atomic Energy of Canada Limited, Chalk River Laboratories, Chalk River, ON, Canada K0J 1J0
[b] National Research Council of Canada, Chalk River Laboratories, Chalk River, ON, Canada K0J 1J0

Received 7 September 2006; accepted 13 February 2007

Abstract

Due to their low absorption cross-section for neutrons, Zr alloys are used for reactor core components. The terminal solid solubility (TSS) for hydrogen in these alloys is very low – in Zr–2.5 wt% Nb, used to fabricate pressure tubes for CANDU (CANDU–CANada Deuterium Uranium is a registered trademark of Atomic Energy of Canada Ltd.) power reactors, the TSS is ~0.7 at.% H at 300 °C. The mechanical properties of the components may deteriorate when their hydrogen concentration exceeds TSS. Therefore, accurate values of the TSS are needed to assess the operating and end-of-life behaviours of these components. Differential scanning calorimetry (DSC) is used to measure the TSS of hydrogen in Zr alloys. Three distinct features are marked on a typical DSC heat flow curve when the material is being heated and the hydrides are dissolving; 'peak temperature', 'maximum slope temperature' and 'completion temperature'. Usually, the maximum slope temperature, being about the average of the three temperatures, is interpreted as the TSS temperature for hydride dissolution (T_{TSSD}). A set of coordinated DSC and neutron diffraction measurements have been carried out to identify the features of the heat flow signal that closely correspond to the T_{TSSD}. Neutron diffraction was chosen because hydrides generate distinctive diffraction peaks whose intensities approach zero at the transition temperature – an unambiguous indication of dissolution. Neutron diffraction shows that the temperature of hydride dissolution correlates closely with the DSC peak temperature.

PACS: 64.70.Kb; 81.30.Bx; 81.30.−t

1. Introduction

Pressure tubes in current CANDU® power reactors are made of cold-worked Zr–2.5Nb (Zr–2.5 wt% Nb) alloy. The microstructure of the tube material consists of elongated α-Zr grains (~90%) surrounded by a network of β-Zr (~10%) with a composition of approximately Zr–20 wt% Nb [1]. The hexagonal close-packed (hcp) α-Zr phase is stable. However, the body-centred cubic (bcc) β-Zr phase is metastable below 620 °C and will gradually transform to α-Zr and β-Nb via intermediate ω and niobium-enriched β-Zr_{enr} phases [2,3]. The pressure tubes operate at an internal pressure of ~10 MPa and temperatures ranging from ~250 °C at the inlet to ~300 °C at the outlet. Over time, these tubes gradually pickup deuterium (D) as a result of corrosion due to exposure to the heavy water (D_2O) coolant. When the hydrogen[1] concentration in the tubes exceeds the terminal solid solubility (TSS), the tubes can become susceptible to a crack propagation process called delayed hydride cracking (DHC). The current database for TSS in zirconium and its alloys shows that the TSS in a given alloy does not have a unique value, but depends on direction of approach to temperature; i.e., on whether hydrides are dissolving (TSSD) or precipitating

* Corresponding author. Tel.: +1 613 584 8811x3662; fax: +1 613 584 8214.
E-mail address: khatamiand@aecl.ca (D. Khatamian).

[1] Reference in the remainder of this paper to hydrogen covers hydrogen and its isotopes, except when specific isotopes are discussed.

0022-3115/$ - see front matter © 2007 Elsevier B.V. All rights reserved.
doi:10.1016/j.jnucmat.2007.02.010

(TSSP). The solubility limit for hydrogen in β-Zr is about one hundred times higher than that in α-Zr [4,5].

Accurate values of the TSS will improve fitness-for-service decisions with regard to DHC susceptibility of pressure tubes in operating nuclear reactors. Several techniques such as diffusion anneal [6], dilatometry [7], acoustic emission [8], metallography [9], dynamic elastic modulus [10], neutron diffraction [11] and differential scanning calorimetry (DSC) [12] have been used to determine TSS in zirconium alloys. Differential scanning calorimetry is a versatile and sensitive technique that requires much smaller specimens than the other methods. This is an advantage because large specimens cannot always be obtained, especially for inspection and monitoring. However, there remain some unresolved issues regarding the interpretation of the DSC signal. The present investigation addresses these issues.

Similar to melting, hydride dissolution in alloys is an endothermic process. There is a measurable change in the amount of heat absorbed by the specimen during the dissolution process. However, unlike melting, hydride dissolution rarely exhibits a well-defined 'sharp' change in the heat flow signal at the transition temperature. Fig. 1 shows a typical heat flow curve obtained from a zirconium specimen during a heating run. Three different temperatures are defined in Fig. 1. In an ideal transition, these temperatures would coincide and the transition would appear as a vertical line. The 'maximum slope temperature' (MST) can be extracted easily, by analyzing the sharp peak in the derivative of the heat flow signal. Traditionally, the MST has been identified as the temperature at which hydride dissolution has completed, TSSD temperature (T_{TSSD}) [12]. However, there is no compelling physical reason to make this identification. In a recent study [4], the hydrogen solubility limit in pure zirconium was examined by DSC. The resulting solubility limits were much lower than the values accepted in the literature when the MST was identified as T_{TSSD}. However, the DSC measurements were found to agree with the accepted solubility data when the 'peak temperature' (PT) was assumed to correspond to T_{TSSD}. It is physically reasonable to identify the PT with the T_{TSSD}, because the trend in the heat flow curve changes direction at this point, i.e., the phase transition is complete. The gradual rise of the heat flow curve after the PT may be explained by the relaxation of the host metal lattice after hydride dissolution. Temperature lag between the sample and the instrument, the temperature gradient across the sample and the heating rate of the sample have also been proposed to explain the apparent difference in the MST compared to the actual value of T_{TSSD}. However, it has been shown [13] that in small metal specimens, typical of DSC measurements, temperature lag and temperature gradients are negligible. It has also been shown that the dissolution temperature is not greatly affected if the heating and the cooling rates in a given thermal cycle (see Section 2.2) are kept similar.

Since DSC is used regularly to measure the hydride dissolution temperature, it is important to remove the uncertainty of interpretation and uniquely identify the feature of the heat flow signal that actually corresponds to the hydride dissolution temperature, T_{TSSD}. Neutron diffraction provides an opportunity to remove this uncertainty because hydrides generate distinctive diffraction peaks whose intensity is directly proportional to the volume fraction of hydride precipitates in the specimen [11]. As the

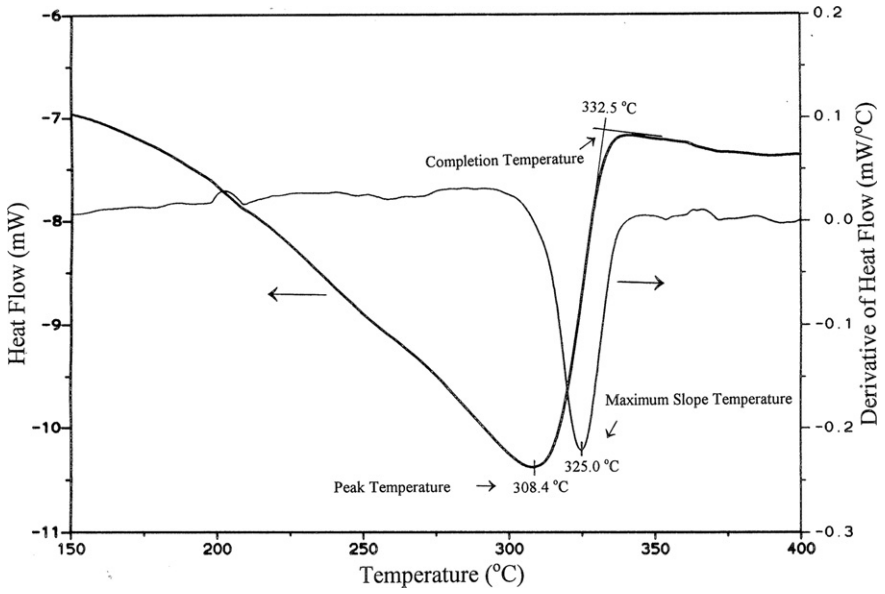

Fig. 1. DSC data from an α-Zr specimen containing 63 ± 3 mg/kg hydrogen obtained during heating. The plot shows the basic heat flow response and its temperature derivative.

temperature is increased, the intensities of hydride diffraction peaks decrease and, at completion of dissolution, they completely vanish. The disappearance of the hydride peak provides an accurate and unambiguous indication of the critical temperature for dissolution, T_{TSSD}. This report focuses on a comparison of neutron diffraction and DSC measurements of T_{TSSD}. The practical implications of these measurements is that if the PT is chosen in the DSC analysis as the T_{TSSD}, the solubility limit for hydrogen in the reactor pressure tubes or any other reactor core components would be notably higher than the presently accepted values, which are obtained using the MST.

2. Experimental

2.1. Specimen preparation

To obtain measurable neutron diffraction patterns from the hydrides present in the specimen, especially close to the transition temperature when the volume fraction of the hydride precipitates approaches zero, one needs to prepare large specimens. Specimens of unalloyed zirconium (α-Zr) and Zr–20 wt% Nb (β-Zr) were charged with deuterium to levels of 220 and 1100 mg D/kg metal, respectively.

The unalloyed zirconium (α-Zr) specimen (10 mm × 10 mm × 50 mm) was analyzed by glow discharge mass spectrometry to determine its impurity levels. The concentrations of the major impurities are given in Table 1. The specimen was blasted with alumina powder, cleaned in an ultrasonic acetone bath and charged with deuterium at 400 °C from the gas phase. The charging process was slow, taking about 3 h. The specimen surface colour was grey, indicating the formation of a solid hydride layer on the surface. The specimen was subsequently annealed at 450 °C for 72 h. A cylindrical specimen of 9 mm diameter and 40 mm height was machined for neutron diffraction experiments. The machining removed residual surface hydride layers. A radial hole at mid-height of the cylinder was drilled to place a Type K thermocouple, which monitored the specimen temperature during the neutron diffraction measurements. A small coupon of ~120 mg was cut for DSC analysis.

The β-Zr specimen (50 mm long × 10 mm diameter) was cut from a Zr–20 wt% Nb rod. The measured niobium concentration was 19.3 wt%. For the concentrations of the major impurities see Table 1. The specimen was initially wrapped in zirconium foil, annealed in vacuum at 850 °C for 1 h and cooled out-of-furnace to transform it to single phase β-Zr [2]. It was then vapour-blasted with alumina powder, cleaned in an ultrasonic acetone bath and charged with deuterium at 400 °C from the gas phase. Due to a much higher solubility limit and diffusivity of hydrogen in β-Zr than in α-Zr [4,5], the charging process was much faster than the α-Zr specimen and it only took ~50 min. After charging, the surface of the specimen looked shiny and metallic, indicating absence of solid surface hydride layers. The specimen was annealed again in a pre-evacuated (~10^{-6} Torr) sealed quartz tube at 850 °C for 1 h to homogenize it and also transform it completely to the β-phase. A small piece of about 100 mg was cut for DSC analysis and the rest was retained for neutron diffraction measurements. A radial hole was drilled at mid-length of the neutron diffraction specimen, for insertion of a type K thermocouple to monitor the sample temperature.

2.2. Differential scanning calorimetry

The DSC measurements were performed with a TA Instruments DSC 2910[2]. This instrument measures the differential heat flow between the specimen and a reference. The heat flow is measured by an area-thermocouple and is recorded for off-line determination of the hydride transition temperature. The DSC instrument is calibrated regularly by a three-point method, using melting points of three standards: indium, tin and lead. For the present work, the reference was a hydrogen-free coupon of the same material and similar size and weight to the specimen. Each specimen was analyzed for the phase transition temperature in several consecutive thermal cycles. The thermal cycles consisted of a heat up from ambient temperature, T_{min}, to some maximum temperature, T_{max}, followed by a cool-down to ambient temperature, with a hold-time of ~5 min at T_{min} and T_{max}. The first thermal cycle served to condition the specimen with a consistent thermal treatment immediately prior to the subsequent cycles. This procedure was adopted to remove the variability in T_{TSSD} that is thought to result from prior handling and treatment of the specimens. If the DSC responses of the latter two thermal cycles were similar, the results were deemed acceptable. In the case of α-Zr specimen, the value of T_{max} for all the thermal cycles was chosen to be 450 °C. However, for the β-Zr specimen T_{max} was kept as low as possible to avoid any transformation of the specimen to ω- or α-phases [3]. In the first thermal cycle T_{max} was 400 °C with no hold-time at T_{max}. In the two subsequent thermal cycles T_{max} was set at 145 °C, which did not provide adequate data to obtain the MST. Therefore, the measurements were continued for a fourth and fifth thermal cycle with T_{max} set at 165 °C. With these experimental parameters and with a heating/cooling rate of 30 °C/min, the specimen was not exposed to temperatures above 300 °C for more than 7 min. Under these conditions, no significant transformation of the specimen should have taken place according to the TTT (temperature–time–transformation) diagram [3]. Following the DSC measurements, both the α-Zr and the β-Zr specimens were analyzed for hydrogen and deuterium concentrations by a Hot Vacuum Extraction Mass Spectrometry (HVEMS) technique [14]. The results are given in Table 2.

[2] TA Instruments Inc., 109 Lukens Drive, New Castle, DE 19720-0311 USA.

Table 1
Major impurities in the α-Zr and β-Zr (Zr–wt% 20Nb) specimens

Sample	Impurity concentration (wt ppm)								
	Oxygen	Iron	Tantalum	Titanium	Carbon	Hafnium	Chromium	Silicon	Nitrogen
α-Zr	340	0.7	0.9	<0.005	18	57	0.02	3	33
β-Zr	1350	520	<200	147	100	<80	<80	<60	50

Table 2
Comparison of the TSS temperatures for dissolution of hydrides in α-Zr and β-Zr (Zr–wt% 20Nb) specimens measured by DSC and neutron diffraction

Specimen	[H] (mg/kg)	[D] (mg/kg)	TSSD temperature (°C)				
			DSC			Neutron diffraction	
			Run number	MST	PT	Run number	T_{TSSD}
α-Zr	6.5 ± 0.6	220 ± 10	1	384 ± 1	359 ± 1	1	361 ± 3
			2	376 ± 1	358 ± 1		
			3	375 ± 1	356 ± 1	2	356 ± 3
			4	376 ± 1	357 ± 1		
			5	375 ± 1	356 ± 1		
			Average	375.7 ± 1[a]	356.8 ± 1[a]	Average	358.5 ± 3
β-Zr	44 ± 2	1020 ± 50	1	150 ± 1	131 ± 1	1	136 ± 2
			2	–	134 ± 1		
			3	–	134 ± 1	2	132 ± 2
			4	146 ± 1	133 ± 1		
			5	146 ± 1	134 ± 1	3	133 ± 2
			Average	146 ± 1[a]	133.8 ± 1[a]	Average	133.7 ± 2

[a] Run number 1 is not included in these averages.

2.3. Neutron diffraction

Each specimen was mounted in a furnace that was designed especially for 'in situ' neutron diffraction measurements. Around the specimen was a cylindrical graphite heater, through which an electric current was passed to generate radiant heat. To minimize thermal gradients in the specimen, the heater volume was evacuated, then back-filled with helium gas at a pressure of approximately 50 kPa to promote conductive heating. As noted earlier, a type-K thermocouple was inserted into the body of each specimen at mid-height to monitor the specimen temperature. A second thermocouple was suspended in the space close to the specimen to provide a responsive signal for controlling the current to the heater. The temperature of the specimen was controlled to a precision of better than ±0.5 °C at each set point. A controlled heating/cooling rate of 2.5 °C/min was applied to change the set-temperature from one value to another. For the present experiment, the data for hydride dissolution were acquired by increasing the temperature stepwise from 47 °C to a maximum temperature of 172 °C for the β-Zr specimen or 407 °C for the α-Zr specimen. The step size varied from ~1.5° (for measurements near the T_{TSSD}) to ~8 °C (away from the T_{TSSD}). The temperature was held constant at each set point, while a neutron diffraction pattern was acquired.

The β-Zr specimen was examined on the L3 neutron diffractometer, at the NRU reactor at Chalk River Laboratories. Diffraction from the (1 1 3) planes of a squeezed, single-crystal germanium monochromator at a take-off angle of 88° produced a neutron beam of wavelength 0.237 nm, which was passed through a pyrolytic graphite filter to suppress higher-order contamination. The incident and diffracted neutron beams were masked to form a sampling volume centred on the specimen, thus reducing background scattering from other materials, such as the various walls and heat-shields inside the furnace. A multi-wire position-sensitive detector collected the complete diffraction peak profile at each temperature. The detector spanned 2.7° of scattering angle, 2θ, centred at 75.0° where a distinctive hydride diffraction peak was found in the β-Zr host metal. The crystal structure of the hydride within the present specimen of β-Zr had been analyzed previously by Rietveld profile refinement with data collected on the C2 neutron powder diffractometer at Chalk River [15]. The structure of the hydride was found to be orthorhombic with lattice parameters $a = 0.3918$ nm, $b = 0.4959$ nm and $c = 0.5018$ nm, space group Pncm, Zr (Nb) atoms at $2a$ and $2c$ sites and hydrogen atoms at $4g$ sites. Therefore, the diffraction peak centred at 75.0° in the current experiment is the (1 1 2) peak of the orthorhombic crystal structure. The full diffraction peak profile of the (1 1 2) hydride peak was collected over a period of 1 h following a

fifteen-minute delay to allow the specimen and furnace to reach thermal equilibrium at each temperature. The (1 1 2) hydride peak is well separated from any of the β-Zr diffraction peaks.

The α-Zr specimen contained zirconium grains with typical dimensions greater than 500 μm, and it was found that the intensity of the (2 2 0) δ-phase hydride peak varied by an order of magnitude on rotating the specimen through 90° about the vertical axis. Additional precautions were therefore needed to obtain reliable diffraction peak data. The specimen and furnace were transferred to the C2 neutron powder diffractometer at the NRU reactor at Chalk River Laboratories. This instrument has an 800-channel, curved, position-sensitive detector that can simultaneously collect data over an 80° range of scattering angle, 2θ, in angular bins separated by 0.1°. The furnace was oscillated continuously through 45° on each side about the vertical axis to sweep as many grains as possible through the diffraction condition and a number of hydride peaks were examined simultaneously in the position-sensitive detector. The wavelength of the neutron beam was 0.237 nm, and a pyrolytic graphite filter was used to suppress higher-order contamination. The incident and diffracted neutron beams were collimated to form a sampling volume centred on the specimen, thus reducing background scattering from the various walls and heat shields inside the furnace. Whereas only one stable hydride forms within the β-Zr phase, two hydride phases were detected in the α-Zr specimen, consistent with known γ and δ structures [11,16,17]. The full diffraction pattern of the α-Zr plus zirconium hydride system was collected, because the $(10\bar{1}0)$ α-Zr diffraction peak is in close proximity to the hydride peaks. The diffraction pattern was collected in eighty minutes, following a ten-minute delay to allow the specimen and furnace to reach thermal equilibrium at each temperature. Suitable hydride peaks were separated from the full diffraction pattern and analyzed as single or double Gaussian peaks.

3. Results

3.1. DSC results

3.1.1. β-Zr matrix

As stated in Section 2.2, the specimen was subjected to a total of five thermal cycles to obtain the required data. The DSC results acquired during a heating part of a thermal cycle are shown in Fig. 2. Fig. 2 shows that the heat flow curve decreases smoothly until the trend changes at 134 °C (PT). It also shows that the MST is at 146 °C. Similar results were also obtained during the other thermal cycles except the first thermal cycle, which, as stated above, was used to condition the specimen. As noted in the experimental section, in cycles 2 and 3, T_{max} was set at 145 °C, which did not provide adequate data to obtain the MST. Therefore, the measurements were continued for two more thermal cycles with T_{max} set at 165 °C. The results from the analyses of all the five thermal cycles are summarized in Table 2.

3.1.2. α-Zr Matrix

The specimen was subjected to five complete thermal cycles and the results for the heating part of the second cycle are shown in Fig. 3. Fig. 3 shows a minimum on the heat flow curve at 357 °C (PT) and a small kink at about 300 °C, which is more pronounced on the derivative of the heat flow curve. The kink, which was absent in the

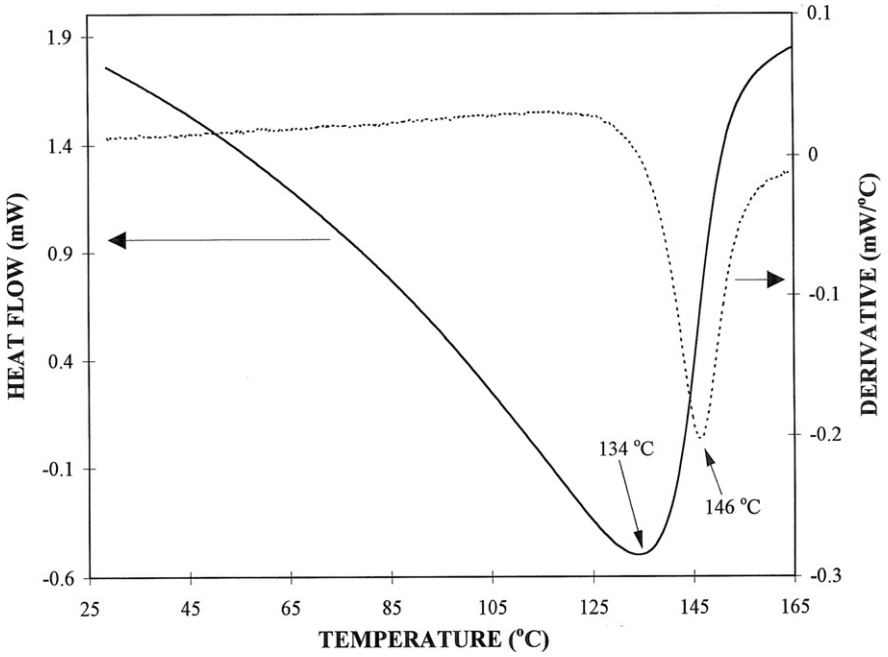

Fig. 2. DSC data from the β-Zr (Zr–20 wt% Nb) specimen obtained during heating. Shown are the basic heat flow response and its temperature derivative.

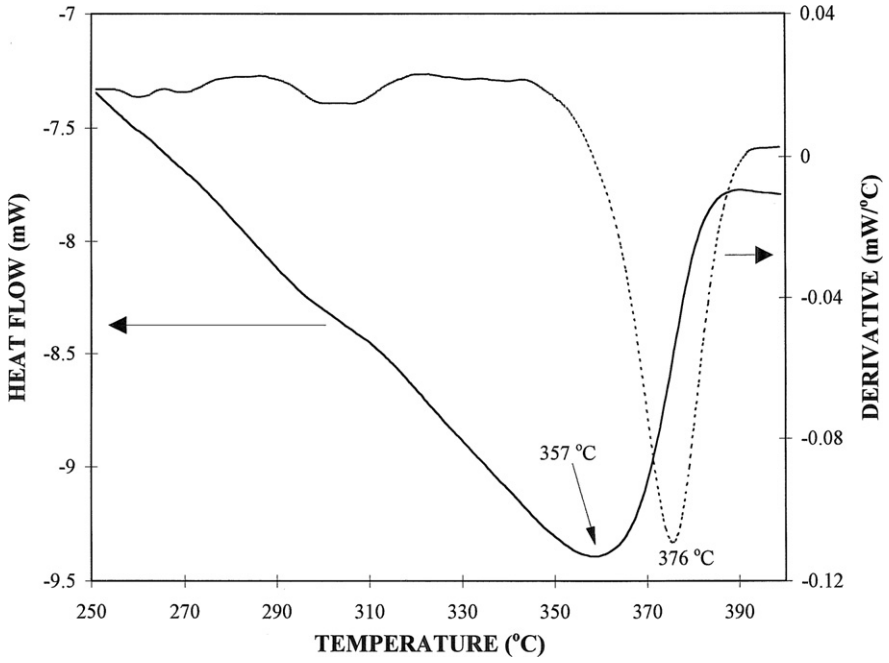

Fig. 3. DSC data from the α-Zr specimen obtained during heating the specimen. Shown are the basic heat flow response and its temperature derivative.

case of the β-Zr specimen, indicates another phase transition in this case and its position appears to coincide with the γ-hydride to δ-hydride transformation (see Section 3.2.2). The MST is at 376 °C. The heat flow curves from the other thermal cycles were similar to these except for the first cycle, which was used to pre-treat the specimen. The results are summarized in Table 2.

3.2. Neutron diffraction results

3.2.1. β-Zr Matrix

The intensity of the (1 1 2) hydride diffraction peak is a reliable indicator of the total volume of hydride precipitates present in the metal matrix at a given temperature. Diffraction peaks at selected temperatures (Fig. 4) illustrate the decrease of intensity with hydride dissolution on heating. The intensity of the diffraction peak can be quantified either by fitting a Gaussian function to the raw data, neutron counts versus scattering angle, and integrating, or by summing the neutron counts over the peak region and subtracting the background counts. The summing method is robust even if the shape of the diffraction peak is not ideal, or if the intensity of the peak is so low that Gaussian fitting cannot be performed. In Fig. 4, the Gaussian fits suggest there is some increase in background counts with temperature, which can be attributed to increased diffuse scattering from the increased vibrational amplitude of atoms in the zirconium crystal structure. At each temperature, the background level was determined by averaging the neutron counts in the first and last two scattering angles of the diffraction peak profile. The average background was subtracted from each neutron count when summing over the diffraction peak to determine the intensity.

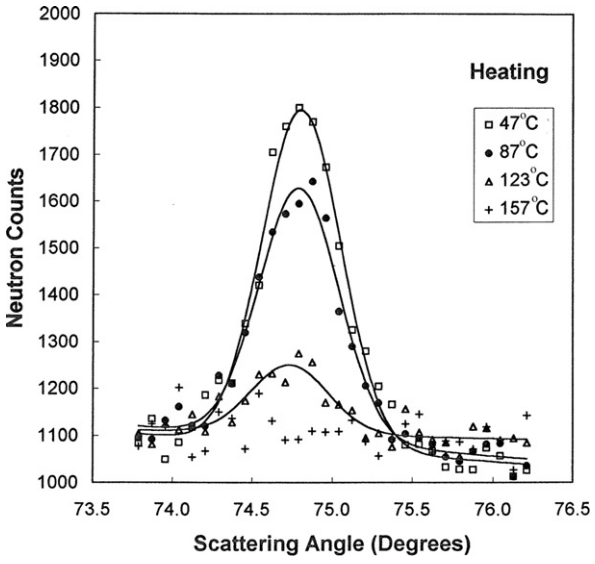

Fig. 4. Variation of the intensity of the (1 1 2) γ-phase hydride peak on heating the β-Zr (Zr–wt% 20Nb) specimen. Continuous lines are Gaussian functions fitted to the raw neutron diffraction data.

The intensity of the (1 1 2) zirconium hydride diffraction peak is plotted in Fig. 5 as a function of temperature, during heating of the specimen. The data below the critical temperature for dissolution are well-represented by the following expression:

$$I_N \propto H_t - C(T), \quad (1)$$

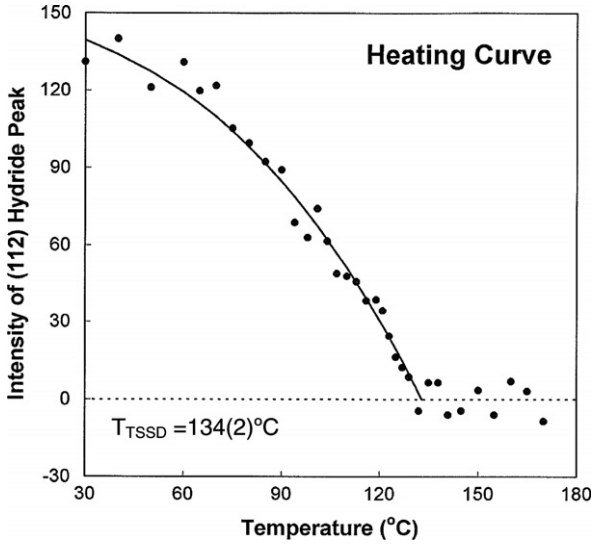

Fig. 5. Temperature dependence of the summed counts in the (1 1 2) diffraction peak on heating of the β-Zr (Zr–wt% 20Nb) specimen. The continuous line indicates the Arrhenius-like function that is fitted to the optimum subset of data points.

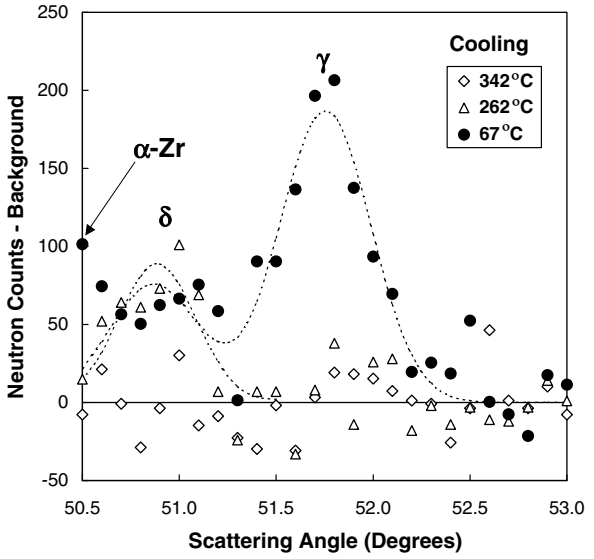

Fig. 6. The variation in shape of the (1 1 1) hydride diffraction-peak doublet on cooling the α-Zr specimen. The $(10\bar{1}0)$ α-Zr diffraction peak is centred at ~50.1° at 67 °C. The high background level has been subtracted from the raw data prior to plotting. Dotted lines are intended as guides to the eye.

where I_N is the total intensity of the neutron diffraction peaks from the hydrides, H_t is the total amount of hydrogen in the sample and $C(T)$ is the amount of hydrogen in solution (solubility limit) at temperature T. The solubility limit, $C(T)$, is given by [18]:

$$C(T) = C_o e^{-Q/RT}, \quad (2)$$

where C_o is a constant, Q is the molar enthalpy of formation and R is the gas constant, 8.314 kJ/mol.

By setting the intensity I_N to zero, the fitted values of H_t, C_o and Q from a heating curve can be combined to estimate the critical temperature for dissolution, T_{TSSD}. The best estimates of the critical temperatures are obtained by fitting Eqs. (1) and (2) to subsets of the data, where points are successively deleted from the high-temperature end. A statistical measure of the goodness-of-fit to the data, χ^2, is evaluated for each subset of data, and the best values of H_t, C_o and Q are extracted from the fit of the subset that yields the lowest value of χ^2. Following this procedure, the critical temperature for the completion of dissolution, T_{TSSD}, was derived for each run. The results are summarized in Table 2.

3.2.2. α-Zr Matrix

In the α-Zr matrix, two hydride phases are detected. The (1 1 1) diffraction peaks of the γ and δ phases are close in scattering angle, but could be resolved with the chosen diffractometer configuration. The growth of hydride precipitates in this system is complicated because at temperatures greater than about 200 °C, the δ-phase predominates and, at lower temperatures, there is a mixture of the two phases. This is illustrated in Fig. 6, where at 342 °C there are no hydrides present, at 262 °C the δ-phase hydride peak has appeared and then at 67 °C both hydride phases are present and the amount of δ-phase appears to be the same as it was at earlier times in the cooling cycle. As previously suggested [11], characterization of the overall dissolution of hydrides, without regard to specific phase, is achieved by plotting the total intensity of the two peaks in the (1 1 1) doublet as a function of temperature. The total intensity is the sum of neutron counts minus background over the measured region. The decrease of total hydride intensity on heating is plotted in Fig. 7 for one of two runs.

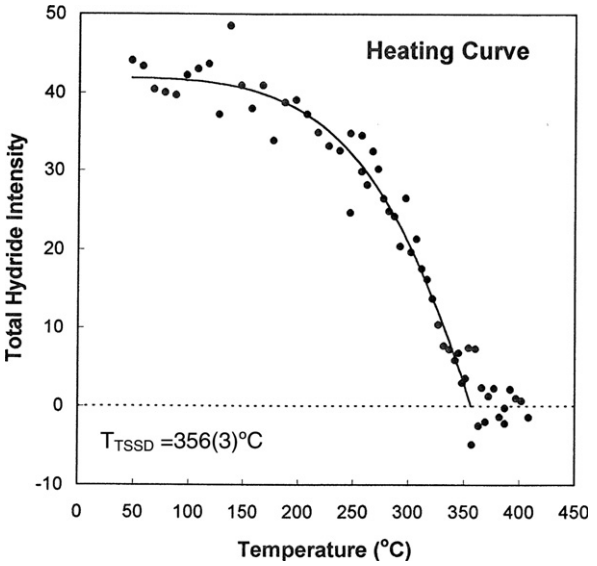

Fig. 7. Temperature dependence of the total summed counts in the (1 1 1) hydride diffraction-peak doublet on heating the α-Zr specimen. The continuous line indicates the fitted Arrhenius-like function.

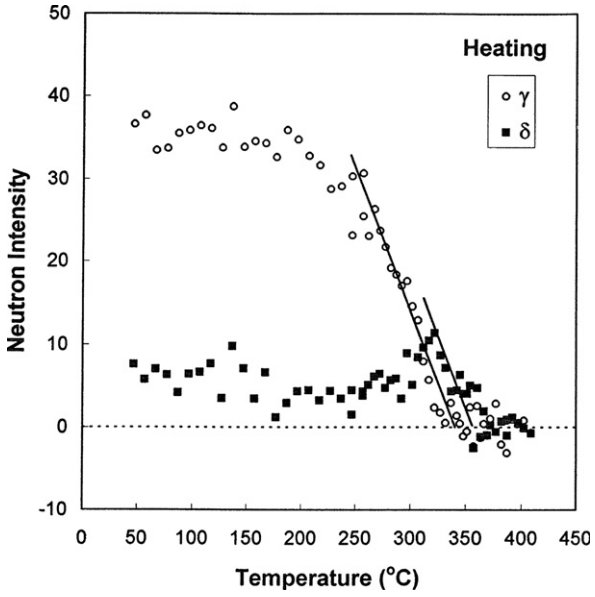

Fig. 8. Separate temperature dependences of the summed counts in the γ- and δ-hydride peaks of the (1 1 1) doublet on heating the α-Zr specimen. Straight lines are guides for the eye, to emphasize that the critical temperatures for dissolution of the two hydride phases are not equal.

Fitting Eqs. (1) and (2) to the data from each run yielded a T_{TSSD}, which is given in Table 2.

It is noted that the individual responses of the γ- and δ-hydride phases to heating or cooling have been considered in a number of thorough investigations of hydride precipitation and dissolution in α-Zr [11,19,20]. The intensities of the (1 1 1) δ- and γ-hydride peaks are determined by summing neutron counts minus background over the appropriate ranges in the diffraction pattern. The variation of intensity on heating is plotted in Fig. 8. At the onset of the heating cycle, the γ-hydride phase predominates. The dissolution of the γ-phase appears to be completed at a temperature that is about 15 °C lower than the T_{TSSD} determined from Fig. 7. Near 300 °C, the intensity of the δ-phase seems to increase slightly, and then persists until the T_{TSSD} is reached.

3.3. Comparison of the DSC and neutron diffraction results

The DSC as well as the neutron diffraction results obtained from both the α- and β-Zr specimens are summarized in Table 2. The table shows that for both specimens the TSSD temperatures obtained using neutron diffraction agree, within the experimental errors, with the DSC 'peak temperature'. This indicates that the DSC peak temperature closely represents the TSSD temperature. The practical implications of this result is that if the peak temperature is chosen in the DSC analysis as the TSSD temperature, the solubility limit for hydrogen in pressure tubes within the reactor operating temperatures (250–310 °C) would be about 7 mg/kg (at 250 °C) to 15 mg/kg (at 310 °C) higher than the currently accepted values obtained using the maximum slope temperature. In other words, the currently accepted values are highly conservative.

4. Conclusions

The hydrogen solubility limits in α-Zr and β-Zr (Zr–20 wt% Nb) samples were measured using DSC and neutron diffraction techniques. These coordinated measurements were carried out to determine the feature of the heat flow signal that actually corresponds to the hydride dissolution temperature. The results, for both the α-Zr and the β-Zr specimens, show that on heating the specimens the hydride dissolution is complete at the DSC peak temperature.

Acknowledgements

The authors wish to thank V.C. Ling for carrying out the DSC measurements, Jim Bolduc, Don Tennant, Larry McEwan and Ron Donaberger for their technical assistance with neutron diffraction measurements and W.A. Ferris for charging the specimens with deuterium. Helpful discussions with A.A. Bahurmuz are acknowledged.

References

[1] D.O. Northwood, X.M. Burany, B.D. Warr, in: C.M. Eucken, A.M. Garde (Eds.), Zirconium in the Nuclear Industry: Ninth International Symposium, ASTM STP, 1132, American Society for Testing and Materials, 1991, p. 156.
[2] J.P. Abriata, J.C. Bolcich, Bull. Alloy Phase Diag. 3 (1982) 1711.
[3] B.A. Cheadle, S.A. Aldridge, J. Nucl. Mater. 47 (1973) 255.
[4] D. Khatamian, V.C. Ling, J. Alloy. Compd. 253 (1997) 162.
[5] A. Sawatzky, G.A. Ledoux, R.L. Tough, C.D. Cann, in: T.N. Veziroglou (Ed.), Proceedings of the Miami International Symposium Metal-Hydrogen Systems, 13–15 April 1981, Miami Beach, FL, p. 109.
[6] J.J. Kearns, J. Nucl. Mater. 22 (1967) 292.
[7] G.F. Slattery, J. Nucl. Mater. 32 (1969) 30.
[8] C.E. Coleman, J.F.R. Ambler, Hydrogen in Metals, Met. Soc. CIM Ann Vol. 17 (1978) 81.
[9] C.D. Cann, A. Atrens, J. Nucl. Mater. 88 (1980) 42.
[10] I.G. Ritchie, Z.L. Pan, in: V.K. Kirna, A. Wolfenden (Eds.), M^3D: Mechanics and Mechanisms of Material Damping, ASTM STP, 1169, American Society for Testing and Material, Philadelphia, 1992, p. 385.
[11] J.H. Root, R.W.L. Fong, J. Nucl. Mater. 232 (1996) 75.
[12] D. Khatamian, Z.L. Pan, M.P. Puls, C.D. Cann, J. Alloy Compd. 231 (1994) 488.
[13] K. Tashiro, private communication, 1994, Ontario Hydro Technologies, Toronto, Ontario, Canada.
[14] G.A. Bickle, L.W. Green, M.W.D. James, T.G. Lamarche, P.K. Leeson, H. Michel, J. Nucl. Mater. 306 (2002) 21.
[15] D. Khatamian, I.P. Swainson, M.J.W. Lucas, J.H. Root, Physica B 241–243 (1998) 1255.
[16] A.I. Kolesnikov, A.M. Balagurov, I.O. Bashkin, A.V. Belushkin, E.G. Ponyatovsky, M. Prager, J. Phys. Condens. Mat. 6 (1994) 8977.
[17] S.S. Sidhu, N.S. Satya Murthy, F.P. Compos, D.D. Zauberis, Adv. Chem. Ser. 39 (1963) 87.
[18] R.A. Swalin, Thermodynamics of Solids, John Wiley, New York, 1962.
[19] W.M. Small, J.H. Root, D. Khatamian, J. Nucl. Mater. 256 (1998) 102.
[20] J.H. Root, W.M. Small, D. Khatamian, O.T. Woo, Acta Mater. 51 (2003) 2041.